

# Shared Promiscuous Activities and Evolutionary Features in Various Members of the Amidohydrolase Superfamily<sup>†</sup>

Cintia Roodveldt and Dan S. Tawfik\*

Department of Biological Chemistry, The Weizmann Institute of Science, 76100 Rehovot, Israel

Received May 31, 2005; Revised Manuscript Received August 1, 2005

**ABSTRACT:** The amidohydrolase superfamily comprises hundreds of hydrolytic enzymes of the ( $\beta/\alpha$ )<sub>8</sub> barrel fold with mono- or binuclear active-site metal centers, and a diverse spectrum of substrates and reactions. Promiscuous activities, or cross-reactivities, between different members of the same superfamily may provide important hints regarding evolutionary and mechanistic relationships. We examined three members: dihydroorotase (DHO), phosphotriesterase (PTE), and PTE-homology protein (PHP). Of particular interest are PTE, which is thought to have evolved within the last several decades, and PHP, an amidohydrolase superfamily member of unknown function, and the closest known homologue of PTE. We found a diverse and partially overlapping pattern of promiscuous activities in these enzymes, including a significant lactonase activity in PTE, esterase activities in both PTE and PHP, and a weak PTE activity in DHO. Directed evolution was applied to improve the promiscuous esterase activities of PTE and PHP. Remarkably, the most recurrent mutation increasing esterase activity in PTE, or PHP, maps to the same location in their superposed 3D structures. The evolved variants also exhibit newly acquired promiscuous activities that were not selected for, including very weak, yet measurable, paraoxonase activity in PHP. Our results illustrate the mechanistic, structural, and evolutionary links between these enzymes, and highlight the importance of studying laboratory evolution intermediates that might resemble node intermediates along the evolutionary pathways leading to the divergence of enzyme superfamilies.

Promiscuous activities have been proposed to play a key role in the evolution of enzymatic functions, by providing a starting point from which new functions may evolve (1–3). Promiscuous activities may also comprise vestiges of the function of the protein from which an enzyme originated, or of its closest evolutionary and mechanistic homologues (for examples, see refs 4–10). Likewise, establishing that one or few mutations can confer a new function to an existing enzyme may indicate that this activity might have been present in its evolutionary ancestors, or might be shared by paralogues that diverged from one same progenitor (4, 11).

The theory that catalytically diverse, yet structurally related, enzymes can arise from divergent evolution is strongly supported by analysis of enzymes possessing the ( $\beta/\alpha$ )<sub>8</sub> barrel (or TIM-barrel) fold (12, 13). The TIM-barrel is the most common enzyme fold reported, accounting for ~10% of structures deposited in the PDB. It is associated with ca. 25 functionally distinct superfamilies (14, 15), most of which are enzymes, implying a versatility of function arising from divergence of enzyme activities. Crystal structures show that the TIM-barrel comprises an 8-fold repeat of  $\beta\alpha$  subunits, with eight parallel  $\beta$ -strands on the inside of the protein forming a cylindrical core, and eight  $\alpha$ -helices on the outside. The active sites of TIM-barrel enzymes are

usually located at the C-terminus of the  $\beta$ -strands, and exhibit a striking similarity within each superfamily (13). The loops connecting the  $\beta\alpha$  units vary between family members and generally comprise the substrate-binding site of each enzyme.

The amidohydrolase superfamily of ( $\beta/\alpha$ )<sub>8</sub> barrel enzymes, in particular, has been well characterized. The most salient structural landmark for this group of predominantly hydrolytic enzymes is a mononuclear or binuclear metal center, whose main role is to activate the substrate for cleavage, and to enhance a hydrolytic water molecule for nucleophilic attack (16). Virtually identical binuclear metal centers are found in phosphotriesterase from *Pseudomonas diminuta* (PTE),<sup>1</sup> urease from *Klebsiella aerogens*, and dihydroorotase (DHO), cytosine deaminase, and phosphotriesterase homology protein (PHP) from *Escherichia coli* (15, 17). Despite this strong similarity, each enzyme catalyzes the hydrolysis of a different substrate and reaction (i.e., the characteristics of the scissile bond are different).

PTE catalyzes the detoxification of a variety of organophosphates (18, 19), although paraoxon is by far its best substrate (Figure 1), with rates approaching the diffusion limit (20). Besides the wide range of phosphotriester substrates

<sup>†</sup> This work was supported by the Israel Science Foundation Bikura grant. D.S.T. is the incumbent of the Elaine Blond Career Development Chair. C.R. was funded by an EMBO short-term fellowship and by the Rodolfo May Scholarship (FGS, The Weizmann Institute of Science).

\* Corresponding author. E-mail: tawfik@weizmann.ac.il. Fax: +972 8 934 4118. Tel: +972 8 934 3637.

<sup>1</sup> Abbreviations: AB, assembly buffer; BA, base analogues; CDFA, carboxyl-diacyetyl fluorescein acetate; DHC, dihydrocoumarine; DHO, dihydroorotase from *Escherichia coli*; Dho, dihydroorotic acid; DMSO, dimethyl sulfoxide; EP, error-prone PCR; IPTG, isopropyl-thiogalactoside; LB, Luria–Bertani medium; MBP, maltose-binding protein; 2NA, 2-naphthyl acetate; PHP, phosphotriesterase homology protein from *Escherichia coli*; PTE, phosphotriesterase from *Pseudomonas diminuta*; TBL, thiobutylolactone; TEBL, 4-thioethyl  $\gamma$ -butyrolactone; wt, wild-type.

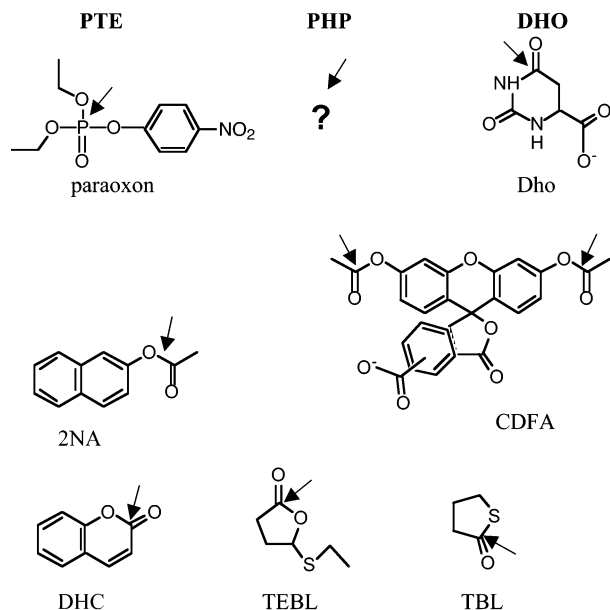


FIGURE 1: Substrates used in this work. PTE's and DHO's native substrates are paraoxon and dihydroorotic acid (Dho), respectively, while the native substrate of PHP is unknown. Promiscuous substrates: esters 2-naphthyl acetate (2NA, the substrate used for selection) and carboxyl-diacyetyl fluorescein acetate (CDFA); lactones dihydrocoumarine (DHC), 4-thio-ethyl butyro-lactone (TEBL), and thiobutyro-lactone (TBL). The arrows indicate the scissile bond.

that have been found to be efficiently hydrolyzed by PTE, traces of thiophosphonate and phosphodiester hydrolyzing activities have been detected (21–23). We have recently reported a promiscuous esterase activity with 2-naphthyl acetate (2NA; Figure 1) (23). However, no naturally occurring substrate for PTE has been identified yet (24), and paraoxon—its “native” substrate as far as turnover rates and substrate recognition are concerned—is a synthetic compound that appeared on this planet in the second half of the 20th century only. This has prompted the suggestion that PTE has evolved in the last few decades from a preexisting hydrolase (19, 24). The closest sequence homologue identified to date is PHP, an enzyme with unknown function, exhibiting 28% sequence identity, and 66% sequence similarity, to PTE. Both enzymes possess an essentially identical binuclear ( $\text{Zn}^{2+}$ ) metal center, and, with the exception of three surface loops, their overall structures superpose quite well (25). These findings suggested that PHP might have been the ancestor of PTE, or that these enzymes diverged from a common progenitor. However, no indication for such evolutionary relationships exists beyond the structural similarity (25, 26).

DHO is a zinc metalloenzyme that catalyzes the reversible interconversion of carbamoyl aspartate and dihydroorotate (27). Dihydroorotase is common to all forms of life and functions in the pathway for the biosynthesis of pyrimidine nucleotides. It was therefore suggested to be closest in function to the most ancient ancestor of the amidohydrolase superfamily (17).

Herein, we describe a diverse pattern of promiscuous activities in PTE, PHP, and DHO, some of which are overlapping. A significant lactonase activity was also found in PTE ( $k_{\text{cat}}/K_{\text{M}} = 160\text{--}6.5 \times 10^5 \text{ M}^{-1} \text{ s}^{-1}$  depending on the substrate), in addition to a significant esterase activity

in both PTE and PHP. These esterolytic activities were substantially improved for both enzymes by directed evolution using 2NA as substrate. Remarkably, the most recurrent and determinant mutation in either PTE (His254Arg) or PHP (Thr210Ala) could be mapped to the same position in their superposed 3D structures. Additional esterase activities, and even a novel paraoxonase activity, emerged along this brief laboratory evolutionary pathway. The PTE and PHP variants identified in the course of our in vitro evolution experiment may therefore represent “node intermediates” with broadened specificity (28, 29), and provide a hint regarding the evolutionary links between these members of the amidohydrolase superfamily.

## MATERIALS AND METHODS

**Expression and Purification of PTE, DHO, PHP, and Variants.** All enzyme variants were overexpressed fused to MBP, and affinity-purified with an amylosed column (NEB) as previously described (23). The purity of the fusion enzymes and their concentrations were established by 12% SDS-PAGE. Small volume analysis of crude lysates was carried out by overexpressing the enzyme variants in 3-mL cultures and lysing cells with 300  $\mu\text{L}$  of BugBuster (Novagen). In either case, enzymes were lysed in the presence of assembly buffer (AB), consisting of 50 mM Tris pH 8.5, 10 mM  $\text{NaHCO}_3$ , and 0.1 mM  $\text{ZnCl}_2$  in the case of PTE, and of 50 mM Tris pH 8.0 and 0.1 mM  $\text{ZnCl}_2$  for PHP and DHO. After purification, the enzymes were extensively dialyzed against their corresponding AB.

**Gene Cloning and Library Construction.** A highly expressing variant of PTE (dubbed PTE-S5) with wild-type-like kinetic parameters (23) was used as a starting point for PTE evolution. Genes encoding PHP (25) and DHO (30) were amplified from *E. coli* DH5 $\alpha$  bacterial colonies with oligonucleotides appending *EcoRI* and *PstI* restriction sites. The amplified genes were subcloned into pMAL-c2x (NEB) predigested with *EcoRI* and *PstI* (NEB).

**Library Construction:** (i) *First-Generation Libraries.* DNA libraries were generated by random mutagenesis either by error-prone PCR (31) using dNTP biases of 4:1 and 10:1 TG/CA (C and A concentrations were each maintained at 0.2 mM) and manganese chloride (0.05 mM), or by the use of 8-oxo-dGTP (1  $\mu\text{M}$  and 5  $\mu\text{M}$ ) as base analogue (BA) introduced into the PCR reaction (32). The libraries were subcloned into pMAL-c2x (NEB) and transformed into *E. coli* DH5 $\alpha$  cells by electroporation for screening and overexpression. Seven randomly chosen clones from each library were used for DNA sequence determination. The average rate of mutation for the EP and BA libraries was  $\sim 2$  per gene.

(ii) *Second- and Third- Generation Libraries.* The variants isolated in the first round of screening were subjected to DNA shuffling (33). Briefly, genes corresponding to the selected variants were amplified using mal E and S1224 primers (NEB). The PCR products were then pooled in equimolar amounts (ensuring that the final gene mixture contained 40% of wild-type genes for “backcrossing”), and incubated with *DpnI* (NEB) to remove the methylated plasmid template DNA. After gel purification (Promega), 10  $\mu\text{g}$  of DNA was digested with DNase I (NEB). DNA

fragments 25–250 bp long were purified by gel electrophoresis (QIAEX II, Qiagen) and assembled by PCR in the absence of primers (33) under the following conditions: 2  $\mu$ g of purified DNA fragments was applied to a 25  $\mu$ L assembly PCR reaction, for which ExTaq DNA polymerase (Takara) was used (34). A variation of this technique was applied for the preparation of second-generation PHP and third-generation PTE libraries, by adding specific oligodeoxynucleotides containing an NNS codon (where N represents any base, and S represents either G or C) at the appropriate position, into the assembly step of the DNA fragments (Hermann and Tawfik, in preparation). Specific oligodeoxynucleotides appending the pMAL-c2x cloning restriction sites *EcoRI* and *PstI* were used for a subsequent nested PCR step, producing DNA that was digested with the cognate restriction enzymes, ligated into predigested pMAL-c2x plasmid, and introduced into *E. coli* DH5 $\alpha$  by electroporation.

**Screening Procedures.** *E. coli* DH5 $\alpha$  cells transformed with the libraries were grown on LB agar plates (containing 100  $\mu$ g mL<sup>-1</sup> ampicillin, 0.5 mM ZnCl<sub>2</sub>, 1% glucose) and replicated as previously described (23, 34, 35) with velvet cloth onto IPTG-containing agar plates, without glucose. After growing at 30 °C overnight, a layer of soft agar supplemented with 2NA (0.3 mM to 0.5 mM) and Fast Red was added (35, 36). Replicates of the most rapidly reddening colonies were inoculated into LB/amp/Zn<sup>2+</sup> (500  $\mu$ L) in 96-deep well plates. Following growth overnight at 30 °C and shaking, the deep-well plates were duplicated, and overexpression was induced by adding IPTG (0.4 mM) and incubating for a further 20 h at 30 °C under shaking conditions. The cultures were centrifuged and the cells were lysed with BugBuster (250  $\mu$ L, Novagen) in AB. Lysates were cleared by centrifugation, and then assayed for hydrolysis of 2NA (0.3 mM) and paraoxon (0.25 mM) as described below. To ensure the monoclonality and verify the activity of the selected variants, the hydrolysis rates were reassayed after growing three subclones in 3 mL from each original colony. Plasmids were extracted and used for mutation analysis and as templates for subsequent rounds of shuffling and screening.

**Determination of Kinetic Constants.** Esterase, phosphotriesterase, and lactonase hydrolysis was followed at ambient temperature by spectrophotometry in 96-well plates with 200- $\mu$ L reaction volumes. Reaction samples for each substrate were all performed at the same fraction of organic solvent. The substrates used (with the monitoring wavelength, extinction coefficient for a 0.5 cm pathway, and final organic solvent content indicated) were 2NA (320 nm,  $\epsilon$  = 600 OD/M, 0.4% methanol), paraoxon (405 nm,  $\epsilon$  = 9200 OD/M, 0.25% methanol), dihydrocoumarine (DHC; 270 nm,  $\epsilon$  = 700 OD/M, 1% DMSO), 4-thio-ethyl butyrolactone (TEBL) containing 0.5 mM 5,5'-dithiobis(2-nitro-benzoic acid) (DTNB) as indicator (412 nm,  $\epsilon$  = 7000 OD/M, 0.5% acetonitrile and 0.5% DMSO; Khersonsky and Tawfik, in preparation),  $\gamma$ -thiobutyrolactone (TBL; 405 nm,  $\epsilon$  = 9200 OD/M, 1% dimethyl sulfoxide), carboxyl-diacetyl fluorescein acetate (CDFA; 490 nm,  $\epsilon$  = 3400 OD/M, 0.3% DMSO), and dihydroorotic acid (Dho; decrease in absorbance at 230 nm,  $\epsilon$  = 855 OD/M). Plots of  $v_0$  vs  $[S]_0$  were fit to the Michaelis–Menten equation  $\{v_0 = k_{cat}[E]_0[S]_0/([S]_0 + K_M)\}$  or to the pseudo-first-order form of it at  $[S]_0 \ll K_M$   $\{v_0 = [E]_0[S]_0k_{cat}/$

Table 1: Specificity Constants ( $s^{-1} M^{-1}$ ) of the Native and Promiscuous Activities of PTE, PHP, and DHO

	activity <sup>a</sup>		
	PTE-S5 <sup>c</sup>	PHP	DHO
paraoxonase	<b><math>(4 \pm 0.8) \times 10^7</math></b>	ND <sup>b</sup>	$2.8 \pm 0.3$
esterase			
2-NA	$480 \pm 40$	$70 \pm 20$	ND
CDFA	$560 \pm 35$	$25 \pm 3$	ND
dihydroorotase	ND	ND	<b><math>(1.2 \pm 0.1) \times 10^6</math></b> <sup>d</sup>
lactonase			
DHC	$(6.5 \pm 0.5) \times 10^5$	ND	ND
EMBL	$(1.14 \pm 0.05) \times 10^3$	ND	ND
TBL	$160 \pm 15$	NA <sup>b</sup>	NA

<sup>a</sup> The native activities are denoted in bold. Results represent the average of two or three independent measurements. Error ranges were calculated from the highest difference between any measured value and the average. <sup>b</sup> ND: not detected. NA: not analyzed. <sup>c</sup> PTE-S5 is a highly expressing variant of PTE with essentially identical kinetic parameters (23). <sup>d</sup> Value taken from ref 27.

$K_M\}$ . The rates of spontaneous hydrolysis for all substrates were subtracted from the corresponding initial velocities. At least two independent measurements were performed for each reaction, using different preparations of the same enzyme variant (i.e., different overexpression and purification batches), and the error range was calculated as the highest difference between any value and the average.

**Inhibition Assays.** The paraoxonase activity of PHP variant 1.1 was competitively inhibited with 2NA using different ratios of both competing substrates (0.3 mM of 2NA and 0.25 mM to 0.75 mM of paraoxon), and simultaneously monitoring the progress in both reactions for 15 min, at 320 and 405 nm, respectively. The data was fit to the following equation:  $V_0(\text{paraoxon})/V_0(2\text{NA}) = (k_{cat}/K_M)_{\text{paraoxon}}[\text{paraoxon}]_0/(k_{cat}/K_M)_{2\text{NA}}[2\text{NA}]_0$  (37).

## RESULTS

**PTE, PHP, and DHO Display an Array of Promiscuous Hydrolytic Activities.** A variety of compounds were examined as substrates for the three enzymes (Figure 1). The esterase and lactonase substrates represent promiscuous hydrolytic activities that have not yet been identified as native functions in the amidohydrolase superfamily. Finally, paraoxon and dihydroorotic acid (Dho)—the native substrates of PTE and DHO, respectively—were tested as potential promiscuous substrates for the noncognate enzymes. Wild-type PHP and DHO were fused to MBP, overexpressed in *E. coli*, purified to homogeneity, and tested with the various substrates. In the case of the PTE, we fused to MBP a variant evolved for higher expression (dubbed PTE-S5) and exhibiting kinetic parameters that are essentially identical to those of wild-type PTE (23).

Our findings are summarized in Table 1. A measurable esterolytic activity was detected for PTE with 2NA, as described before (23). We also detected a modest activity for PHP with this substrate ( $k_{cat}/K_M$  48  $s^{-1} M^{-1}$ , Figure 2a). Previous studies indicated no esterolytic activity of PHP toward *p*-nitrophenyl acetate (PNPA) (25). It is likely that the high spontaneous hydrolysis rate of PNPA masked the low-level esterolytic activity. PTE and PHP also share a significant hydrolytic activity with another ester (CDFA). Unexpectedly, a significant lactonase activity was identified in PTE, not only with the activated aromatic lactone DHC



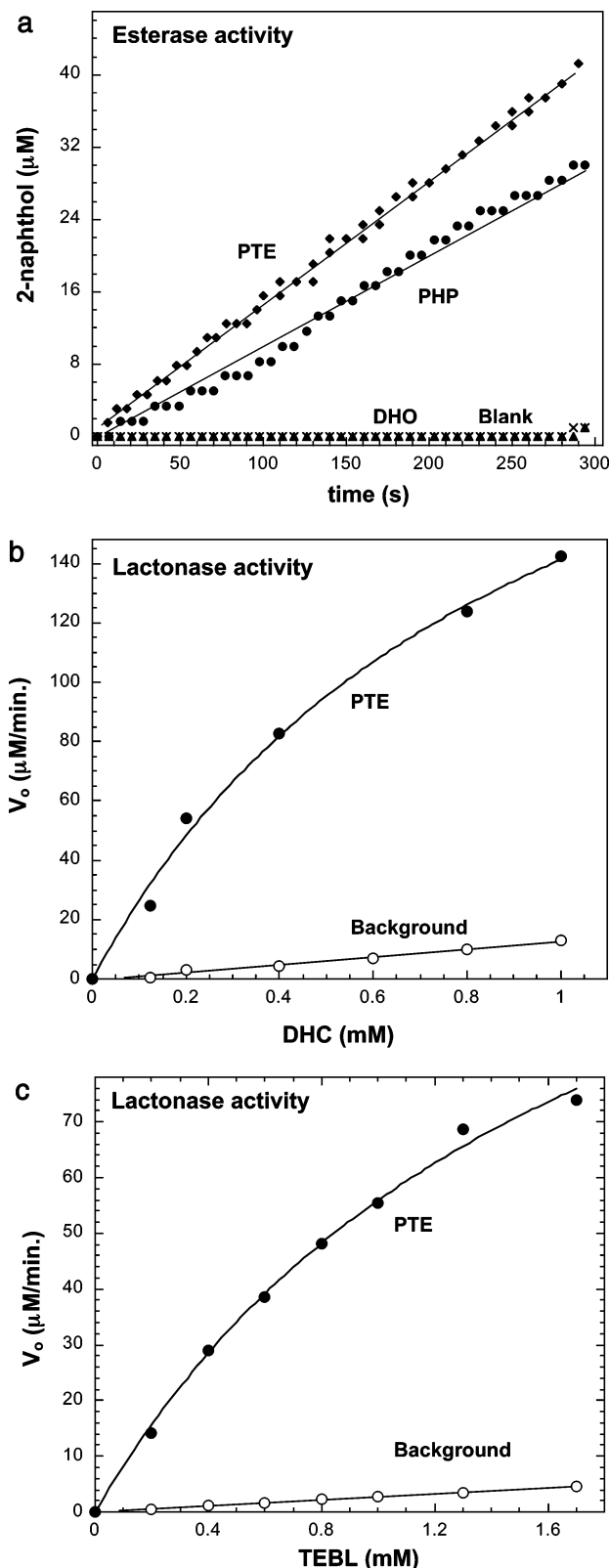


FIGURE 2: Identification of promiscuous activities in PTE and PHP. (a) The esterase activity assayed with 2-naphthyl acetate (2NA, 0.3 mM) for PHP ( $[E]_0 = 4 \mu\text{M}$ ; pH 8.0), PTE-S5 ( $0.9 \mu\text{M}$ ; pH 8.5) and DHO ( $[E]_0 = 2 \mu\text{M}$ ; pH 8.0). (b, c) Michaelis–Menten analysis of the lactonase activities of PTE-S5 with DHC and TEBL (pH 8.0;  $[E]_0 = 7 \text{ nM}$  and  $1.25 \mu\text{M}$ , for DHC and TEBL, respectively).

( $k_{\text{cat}}/K_M = 6.5 \times 10^5 \text{ s}^{-1} \text{ M}^{-1}$ , Figure 2b) but also with a nonactivated lactone (TEBL;  $k_{\text{cat}}/K_M = 1.1 \times 10^3 \text{ s}^{-1} \text{ M}^{-1}$ , Figure 2b) and with the thiolactone TBL ( $160 \text{ s}^{-1} \text{ M}^{-1}$ ).

Finally, DHO exhibited a low yet measurable paraoxonase activity ( $k_{\text{cat}}/K_M = 2.8 \text{ s}^{-1} \text{ M}^{-1}$ ).

The reliable detection of very low promiscuous activities requires adequate controls. In a sense, having three different enzymes that were overexpressed and purified under exactly the same conditions served as an internal control in these assays. The patterns of promiscuous activities displayed by these enzymes seem to be singular. For example, no paraoxonase, lactonase, or dihydroorotase activities were detected for PHP, and DHO displayed no esterase activity. In addition, the esterase and lactonase activities of PTE were inhibited ( $K_i$  of 1.35 mM and 1.2 mM, respectively; data not shown) by diethyl phenyl phosphate, an extremely slow substrate of PTE with a  $k_{\text{cat}}$  of  $0.01 \text{ s}^{-1}$  and a  $K_M$  value (3.5 mM (38)) that is in the range of the  $K_i$  obtained. This indicates that the promiscuous activities are catalyzed by the very same active site. Similarly, the paraoxonase activity of DHO was competitively inhibited by its native substrate, dihydroorotic acid (data not shown). However, given that a significant amount of enzyme is necessary to detect the low level paraoxonase activity, it was only possible to observe the inhibitory effect of the native substrate during the first few minutes of reaction, i.e., before the native substrate has been exhausted. Finally, although no native substrate or ligand for PHP is known, we could show that a new promiscuous activity that appeared in PHP variants (see Figure 4 below) was competitively inhibited by another promiscuous substrate. Thus several independent results demonstrate that these alternative reactions are mediated by the same active sites.

**Directed Evolution for Esterase Activity.** Having established an array of promiscuous activities for PTE, PHP, and DHO, we wanted to examine potential evolutionary pathways leading to higher proficiency of the activities. Random mutagenesis libraries were generated both by error-prone PCR (31) and base analogues (32), with an average mutation rate of  $\sim 2$  substitutions per gene. A wild-type-like PTE variant (PTE-S5) served as starting point (23) alongside the wild-type genes encoding DHO and PHP. We then performed colony screens with 2NA (23) of approximately 20 000 colonies from each library ( $\sim 40$  000 per gene, in total).

Screening of PTE libraries produced 150 positive agar colonies in the first round. Twenty-three of these clones were regrown in liquid medium, lysed, and reassayed with 2NA. One particular mutation, His254Arg, was identified in most selected variants (Table 2). Fifteen nonredundant, first-round variants exhibiting the highest esterase activity were recombined by DNA shuffling in the presence of the PTE-S5 gene. This second-round library was screened, yielding active esterase variants 2.1, 2.2, and 2.4 (all three containing the His254Arg substitution), that exhibited significant improvements over PTE-S5 (Table 2). To make sure that the His254Arg mutation increases the activity independently of the three mutations present in PTE-S5 (responsible for increasing functional expression (23), the His254Arg substitution was incorporated into wtPTE. As expected, this single mutation by itself mirrored the measured improvements in activity seen in the PTE-S5 variants, for all tested substrates (see Table 3 footnote c). With the aim of improving these activities further, third-generation PTE libraries were built using two different strategies: random mutagenesis by error-prone PCR of the best three PTE

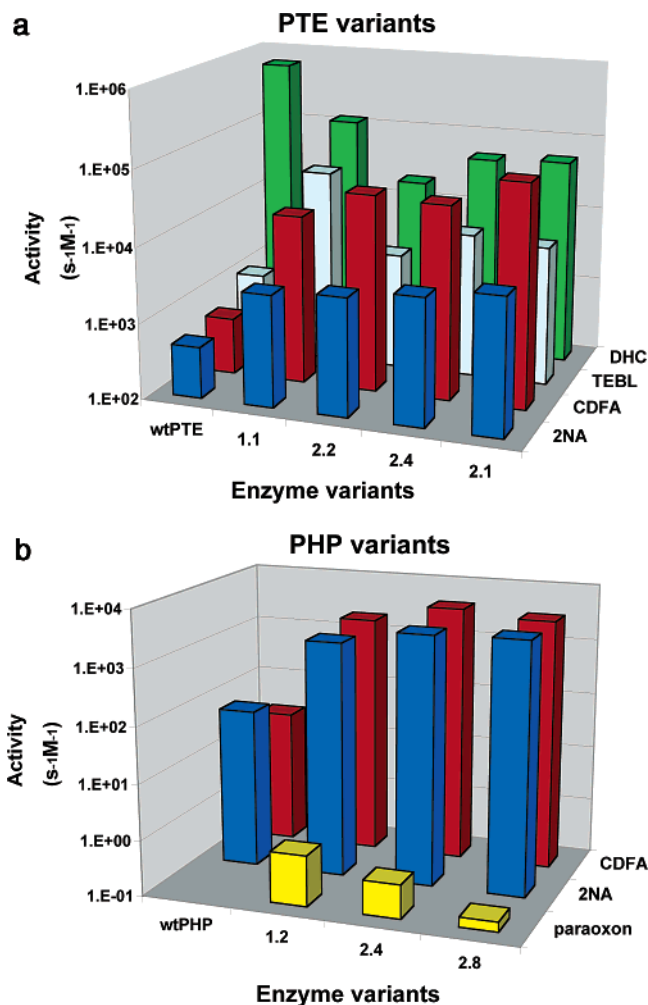


FIGURE 3: Histograms representing the specificity constants ( $k_{\text{cat}}/K_M$ ) for the promiscuous activities of the evolved PTE and PHP variants with different substrates.

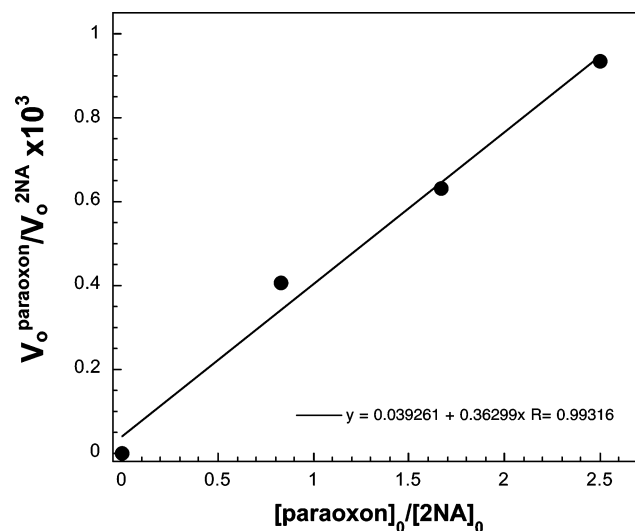


FIGURE 4: The relative rates of the evolved PHP variant 1.2's paraoxonase and esterase activities with 2NA indicate that both reactions are catalyzed by the same active site. The slope of the line corresponds to the ratio between the specificity constants ( $k_{\text{cat}}/K_M$ ) of both reactions measured independently (Table 3).

variants, and saturation mutagenesis of the His254 codon with an NNS variable codon (N represents an equimolar mixture of all bases; S represents an equimolar mixture of

Table 2: Mutations Identified in the Selected PTE-S5 and PHP Variants

PTE variant	T45	V84	A176	H254	Q290	F306	V320	P342
1.1 <sup>a</sup>				R				
1.2		A		R				
1.3	A				R	C		
2.1				R		C		A
2.2			V	R		C		
2.3				R		C	A	
2.4			V	R		C		A
3.1			V	R <sup>b</sup>		C		
3.2				R		C		

PHP variant	K23	A87	T183	T210	T245
1.1 <sup>a</sup>	T				
1.2				A	A
2.1	S			A	
2.2	T			A <sup>b</sup>	
2.3	Y			C	
2.4	Y			A	A
2.5	L		I	T <sup>b</sup>	A
2.6	D		I	A	A
2.7	H	G		C	
2.8	Y		I	T <sup>b</sup>	A
2.9	T		I		A

<sup>a</sup> The first number indicates the round of screening. <sup>b</sup> Although the selected amino acid was arginine, alanine, or threonine, the codon differs from either wild-type, or that selected in the first round of screening.

G or C). Screening of these libraries produced variants exhibiting yet higher activity. However, after analyzing the lysates of the overexpressed variants, it was noticed that the higher rates were due to increased expression levels.

The PHP libraries rendered a total of 420 potential positive clones in the first round. These were transferred to liquid medium in 96-deep-well plates, and lysates prepared and assayed for 2NAase and paraoxonase activities. Thirty clones were selected from this screen and regrown in liquid medium, lysed, and reassayed with 2NA. Of these, variant PHP 1.2 was the most active esterase. Sequencing of improved variants identified two specific amino acid positions that appeared to be favored: Thr210 and Lys23. We then diversified these two positions with NNS codons, using, as template, either wt PHP or the shuffling products of the best first-round variants. In the latter case, wt PHP was also included in the DNA shuffling reaction. Both libraries generated variants with higher esterase activities, but the best results were obtained with the shuffled library, which yielded yet higher improvements in activity (Table 2).

In contrast to PTE and PHP, screening of the DHO libraries did not yield any variant with measurable esterase activity. This result is not surprising given that the starting point, wt DHO, exhibits no esterase activity.

**Characterization of the Evolved PTE Variants.** The vast majority of the selected PTE variants contained a His254Arg substitution, either as a single mutation or combined with other substitutions, mainly Ala176Val, Phe306Cys, and Pro342Ala (Table 2). Screening of the third-generation library reproduced the second-round variants with additional silent mutations, suggesting that the esterase activity had evolved toward its optimum under the dynamic range of the screen.

Several variants were affinity-purified using the MBP fusion tag, and analyzed in detail. The catalytic performance of the PTE first-round intermediate 1.1, and of second-round

Table 3: Kinetic Constants of Evolved PTE and PHP Variants

PTE variant	2NA	CDFA	paraoxon			DHC	TEBL
	$k_{\text{cat}}/K_M$ ( $\text{s}^{-1} \text{M}^{-1}$ ) <sup>a,b</sup>	$k_{\text{cat}}/K_M$ ( $\text{s}^{-1} \text{M}^{-1}$ )	$k_{\text{cat}}$ ( $\text{s}^{-1}$ )	$K_M$ ( $\mu\text{M}$ )	$k_{\text{cat}}/K_M$ ( $\text{s}^{-1} \text{M}^{-1}$ )	$k_{\text{cat}}/K_M$ ( $\text{s}^{-1} \text{M}^{-1}$ )	$k_{\text{cat}}/K_M$ ( $\text{s}^{-1} \text{M}^{-1}$ )
PTE-S5 <sup>c</sup>	480 ± 40	560 ± 35	(2.15 ± 0.2) × 10 <sup>3</sup>	55 ± 6	4.1 × 10 <sup>7</sup>	(6.5 ± 0.5) × 10 <sup>5</sup>	1140 ± 50
1.1	(3.0 ± 0.3) × 10 <sup>3</sup> <b>(6.3)<sup>d</sup></b>	(1.7 ± 0.1) × 10 <sup>4</sup> <b>(30.4)</b>	354 ± 10 <b>(0.16)</b>	5 ± 0.5 <b>(0.09)</b>	6.9 × 10 <sup>7</sup> <b>(1.7)</b>	(1.2 ± 0.2) × 10 <sup>5</sup> <b>(0.18)</b>	(3.8 ± 0.2) × 10 <sup>4</sup> <b>(33.2)</b>
2.2	(3.6 ± 0.3) × 10 <sup>3</sup> <b>(7.5)</b>	(4 ± 0.3) × 10 <sup>4</sup> <b>(71.5)</b>	580 ± 5 <b>(0.3)</b>	95 ± 5 <b>(1.7)</b>	6.1 × 10 <sup>6</sup> <b>(0.15)</b>	(2.0 ± 0.3) × 10 <sup>4</sup> <b>(0.03)</b>	(3.5 ± 0.1) × 10 <sup>3</sup> <b>(3.1)</b>
2.4	(4.7 ± 0.4) × 10 <sup>3</sup> <b>(9.7)</b>	(3.6 ± 0.1) × 10 <sup>4</sup> <b>(64.3)</b>	867 ± 20 <b>(0.4)</b>	115 ± 5 <b>(2.1)</b>	7.2 × 10 <sup>6</sup> <b>(0.18)</b>	(5.0 ± 0.4) × 10 <sup>4</sup> <b>(0.08)</b>	(8.2 ± 1) × 10 <sup>3</sup> <b>(7.2)</b>
2.1	(6.2 ± 0.5) × 10 <sup>3</sup> <b>(12.9)</b>	(8.5 ± 0.9) × 10 <sup>4</sup> <b>(152)</b>	980 ± 20 <b>(0.46)</b>	80 ± 5 <b>(1.45)</b>	1.2 × 10 <sup>7</sup> <b>(0.3)</b>	(5.5 ± 0.6) × 10 <sup>4</sup> <b>(0.08)</b>	(6.9 ± 0.7) × 10 <sup>3</sup> <b>(6.1)</b>
PHP variant	2NA	CDFA	paraoxon		DHC		
	$k_{\text{cat}}/K_M$ ( $\text{s}^{-1} \text{M}^{-1}$ ) <sup>a,b</sup>	$k_{\text{cat}}/K_M$ ( $\text{s}^{-1} \text{M}^{-1}$ )	$k_{\text{cat}}/K_M$ ( $\text{s}^{-1} \text{M}^{-1}$ )	$k_{\text{cat}}/K_M$ ( $\text{s}^{-1} \text{M}^{-1}$ )	$k_{\text{cat}}/K_M$ ( $\text{s}^{-1} \text{M}^{-1}$ )		
wtPHP	70 ± 20	25 ± 3	ND	ND <sup>e</sup>	ND		
1.2	(1.6 ± 0.16) × 10 <sup>3</sup> <b>(23)<sup>d</sup></b>	(2.01 ± 0.15) × 10 <sup>3</sup> <b>(81)</b>	0.8 ± 0.1 2.3 ± 0.2 <sup>e</sup>		ND		
2.4	(2.87 ± 0.13) × 10 <sup>3</sup> <b>(41)</b>	(4.1 ± 0.3) × 10 <sup>3</sup> <b>(164)</b>	0.4 ± 0.05		ND		
2.8	(3.1 ± 0.18) × 10 <sup>3</sup> <b>(44)</b>	(3.17 ± 0.13) × 10 <sup>3</sup> <b>(127)</b>	0.15 ± 0.05		ND		

<sup>a</sup> Results represent the average of two or three independent measurements. <sup>b</sup> Error ranges were calculated as the highest difference between any value and the average. <sup>c</sup> The His254Arg substitution was incorporated into wtPTE. As expected, this single mutation mirrors the improvements in activity seen in the PTE-S5 variant, as follows: 2NA, 7-fold; CDFA, 35-fold; TEBL, 17-fold; paraoxon, 1.6-fold ( $k_{\text{cat}} = 192 \text{ s}^{-1}$ ;  $K_M = 3.0 \mu\text{M}$ ). <sup>d</sup> Variations in activities relative to wild-type are indicated below in bold letters. <sup>e</sup> All kinetic parameters correspond to the  $\text{Zn}^{2+}$ -assembled enzyme. The activities of  $\text{Co}^{2+}$ -assembled PHP variants were also tested, and the rates with paraoxon are noted in the second line.

2.1, 2.2, and 2.4 variants, was assayed with 2NA—the screening substrate—and with paraoxon, PTE’s “native” substrate. Due to the limited aqueous solubility of 2NA, the  $k_{\text{cat}}$  and  $K_M$  parameters could not be determined, and  $k_{\text{cat}}/K_M$  values were deduced under pseudo-first-order conditions ( $[\text{S}]_0 \ll K_M$ ). As can be observed (Table 3, Figure 3a), ca. 13-fold improvement was obtained for the second-round variant 2.1, while the 1.1 intermediate displayed ca. 6-fold improvement. In agreement with the behavior described for PTE variant 2.1 (29), the activity with paraoxon for the three second-round PTE variants was similar to that of wild-type PTE-S5. In the case of variant 1.1 carrying the single His254Arg mutation (Table 2), a significant reduction in  $k_{\text{cat}}$  (from  $2150 \text{ s}^{-1}$  to  $354 \text{ s}^{-1}$ ) and a concomitant reduction in  $K_M$  (from  $55 \mu\text{M}$  to  $5 \mu\text{M}$ ) gave a  $k_{\text{cat}}/K_M$  value that is also very similar to the starting point PTE-S5 (Table 3). As indicated (Table 3), this mutation has the same effect on wtPTE.

The selected variants were also tested with a variety of other substrates that were not screened for. A 150-fold increase in activity was recorded with CDFA ester (Table 3). On the other hand, the lactonase activity with DHC decreased progressively along evolution, while rates of TEBL hydrolysis for the evolved variants increased, notably in the case of the PTE 1.1 intermediate (Table 3, Figure 3a).

**Characterization of Selected PHP Variants.** In the case of the PHP evolved mutants, a trend similar to that of PTE was observed (Table 2). Even though, relative to PTE, a larger variety of mutations arose from the first round of selection, Thr210Ala was predominant, either in isolation, or combined with another one, typically Thr245Ala. Position Lys23 was also mutated in some clones, generally in isolation. Interestingly, this residue was found mutated to four different amino acids: Asn, Glu, Thr, and Ser. The

screening of the second-generation library produced active variants with different residues at position Lys23, usually in combination with Thr210Ala or Thr210Cys, Thr245Ala, and Thr183Ile, which was not observed in the first round. Interestingly, the original Thr210Ala mutation was reverted back to Thr in PHP 2.8 (Table 2).

Analysis of the purified PHP variants indicated a 23-fold improvement in 2NA esterase activity variant 1.2, and a 44-fold higher activity for the second-round variant 2.8 (Table 3, Figure 3b). Even higher improvements were observed with CDFA as substrate (Table 3, Figure 3b). An unexpected low level of paraoxonase activity (ranging from  $0.15$  to  $0.8 \text{ s}^{-1} \text{M}^{-1}$ ) appeared in the evolved PHP variants despite its absence in the wild-type enzyme (Table 3, Figure 3b). To ensure that the paraoxonase activity is catalyzed by the same active site that accelerates the esterase reaction, evolved PHP variant 1.2 was allowed to simultaneously react with both substrates along a range of concentrations (Figure 4). As anticipated for the case of two substrates competing for the same active site (37), a plot of the ratio of initial rates observed with each of the two substrates versus the ratio of their concentrations gave a linear line, the slope of which corresponds to the ratio of  $k_{\text{cat}}/K_M$  for these substrates (2750 vs 2100, the ratio obtained from the independently measured  $k_{\text{cat}}/K_M$  values, Table 3).

## DISCUSSION

**The Selected Mutations in PTE and PHP.** Residues that determine the substrate specificity and catalytic activity in the  $(\beta/\alpha)_8$  barrel enzymes are often contributed either from the C-terminal ends of the  $\beta$  strands of the barrel or from the loops connecting the strands with the  $\alpha$ -helices that follow them (25, 39). In the amidohydrolase superfamily members in particular, loops 7 and 8 are most often involved



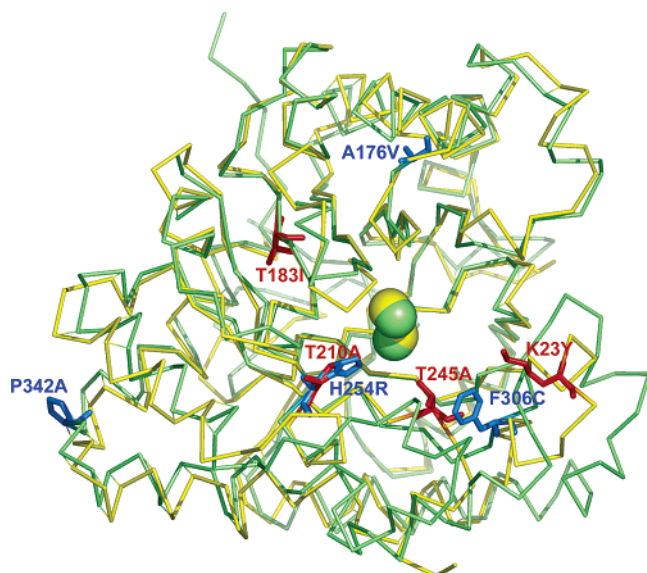


FIGURE 5: Overlaid backbone structures of PTE (lime) and PHP (yellow). The two  $\text{Zn}^{2+}$  ion pairs are represented as spheres. The mutations observed in the selected variants are denoted for PTE (blue) and PHP (red). Note the overlapped location of PTE 254 and PHP 210 positions.

in contacting the ligands in the active site and determining substrate specificity (16). Indeed, these are the loops in which PHP and PTE differ most (25). Interestingly, the key mutations leading to higher esterase activity are located in these loops.

The His254Arg mutation was identified in almost all the selected PTE variants (Table 2), and seems to be of general significance. His254 has been shown to interact through a hydrogen bond with the direct metal-ligating residue Asp301 from strand 8 (40), and may facilitate the shuttling of protons away from the active site of PTE during substrate turnover (41). In the highly homologous organophosphate-degrading enzyme from *Agrobacterium radiobacter* (OPDA; 90% identity to PTE), position 254 corresponds to an Arg residue that appears to undergo a substrate-induced conformational change and stabilize one of the phosphate oxygens of the substrate (42). The His254Arg substitution was also observed in variants of PTE evolved for higher activity with coumaphos-o-analogue (42), and with phosphothiolate substrates. In the latter context, the His254Arg variant was crystallized (pdb: 1qw7 (43)). We have overlaid the structures of the His254Arg mutant with that of wild-type PTE (pdb: 1hzy (44)) and observed that they superimpose almost perfectly, apart from a subtle deviation ( $\sim 1.2$  Å) of the backbone in the turn connecting  $\alpha$ -helix 8 with  $\alpha$ -helix 8', a region that is quite remote from the active site. Interestingly, two of our selected PTE variants contain, in addition to His254Arg, a Pro342Ala mutation (Table 2; PTE variants 2.1 and 2.4). Residue 342 is located precisely at this turn, implying a possible role for the Pro342Ala mutation in alleviating the backbone distortion induced by the His254Arg mutation.

The key mutations, PTE His254Arg and PHP Thr210Ala, occur at overlapping positions in the two structures, and this position is located in the active site, at the region between the C-terminus of strand 7 and the  $\beta$ - $\alpha$  loop 7 (Figure 5). This result provides further support to the hypothesis that PTE and PHP are structurally and evolutionary related (26). It also indicates that mutations conferring new substrate

selectivities occur at key positions that are probably characteristic to each family within a large superfamily.

Other mutated residues include Phe306, which is located at the N-terminus of loop 8 of PTE and close to its active site, and has been suggested to be critical for the maintenance of its structural integrity (45). In the PHP evolved variants, the Thr245Ala mutation is also located in loop 8, which is significantly shorter than in PTE (Figure 5) (26). While the key mutations were mapped to loops 7 and 8 as discussed above, several mutations were found in other regions. Positions Pro342 (see above) and Ala176 in PTE are very remote from the active site, while in PHP Lys23 is located in loop 1, and Thr183 lies at the C-terminus of strand 6. However, unlike the loop 7 and 8 mutations, the effect of these substitutions on the various enzymatic activities is relatively minor.

*Promiscuity and Divergence of New Functions in a Superfamily.* We provided a detailed description of the promiscuous activities in three different members of the amidohydrolase superfamily (Table 1). Some of the activities are performed by only one enzyme, e.g., only PTE exhibits lactonase activity, and others are shared by more than one (e.g., both PTE and PHP exhibit esterase activities). In line with the findings of others (5–9, 26), the native activity of one member can be promiscuously catalyzed by another family member (e.g., DHO exhibits promiscuous PTE activity).

Our results also emphasize how easily new function can diverge within a superfamily while maintaining the overall architecture, active site features, and the basic mechanism of catalysis (12, 15–17). Variants of  $(\beta/\alpha)_8$  barrel enzymes containing a few, or even single, mutations have been previously isolated in the laboratory, resulting in a higher proficiency of an initially low promiscuous function, or leading to new substrate specificities (46, 47). For example, L-Ala-D/L-Glu epimerase (AEE) and muconate lactonizing enzyme (MLE II) variants belonging to the enolase superfamily of  $(\beta/\alpha)_8$  barrel enzymes have been engineered or evolved *in vitro* for a higher *o*-succinylbenzoate synthase (OSBS) activity, which is present in the evolutionarily related OSBS member of the superfamily (11). The selected variants were capable of efficiently catalyzing a mechanistically different reaction by introduction of a single mutation. In all these cases (5, 11, 46, 47), the evolved or engineered enzymatic function corresponded to the native activity of another superfamily member. The results presented herein show that two members of the amidohydrolase superfamily, PTE and PHP, are capable of adopting considerable esterase activity with only a few—even single—substitutions. Although esterase has not been so far identified as a native function in any other member of the amidohydrolase superfamily, it is mechanistically similar to other hydrolytic reactions catalyzed by the members of this group of metalloenzymes. It is therefore likely that TIM-barrel metalloesterases identified in the future may belong to this superfamily, or that this activity could be further evolved in the laboratory to expand the range of substrates and reactions that are catalyzed by amidohydrolases.

*The Evolutionary Origins of PTE.* As described in the introduction, there are several indications that PTE has evolved in the last few decades from a preexisting hydrolase (19, 24–26). The closest sequence homologue identified to

date is PHP, exhibiting 28% sequence identity, 66% sequence similarity, and considerable structural homology to PTE (25, 26). Albeit, the native substrate of PHP is unknown, and previous studies have shown that it does not possess paraoxonase activity. Thus, no functional indications for a link between PTE and PHP existed thus far. Here we show that PHP shares a promiscuous esterase activity with PTE, and that the esterase activities of the enzymes can be increased following a mutation that occurs at the very same active site location (Figure 5). Further, mutants of PHP with increased esterase activity also show a measurable (although very weak) paraoxonase activity. This study also indicates a rather pronounced lactonase activity in PTE with  $k_{\text{cat}}/K_M$  values of  $160\text{--}6.5 \times 10^5 \text{ M}^{-1} \text{ s}^{-1}$  observed with different lactones and thiolactones (Table 1). In addition, few mutations were identified that significantly increase the activity of PTE with certain lactones (Table 3). This observation is hard to interpret at this stage, but the future identification of amidohydrolases with lactonase activity may provide the missing link between a newly evolved PTE and older members of this highly diverse superfamily.

**Multispecific Enzymes and Evolutionary Intermediates.** It was previously shown that the selection of variants for an increase in one promiscuous activity led to evolutionary intermediates that exhibited broadened specificity and were capable of catalyzing a range of substrates that were not selected for (11, 28, 48–50). Similar results were obtained here with PHP variants that were selected toward higher esterase activity and displayed measurable rates of paraoxon hydrolysis, an activity that was not detected in wild-type PHP (Table 3) (26). Matsumura and Ellington proposed that only relatively few mutations are usually required to convert natural “specialists” into “generalists” (28). Indeed, most evolved variants are, at the early steps of the evolutionary process, multispecific, or “generalists” because they have gained new activities but still maintain their native ones (29). The results presented here illustrate the case of “node evolutionary intermediates” in which not only new specificities but even novel activities can emerge. Such intermediates, with myriad promiscuous activities and largely unaffected native function, may resemble evolutionary progenitors (4, 28).

## ACKNOWLEDGMENT

C.R. would like to thank Dr. Stephen McQ Gould and Dr. Sergio Peisajovich for their useful comments on the manuscript.

## REFERENCES

- Jensen, R. A. (1976) Enzyme recruitment in evolution of new function, *Annu. Rev. Microbiol.* 30, 409–25.
- O'Brien, P. J., and Herschlag, D. (1999) Catalytic promiscuity and the evolution of new enzymatic activities, *Chem. Biol.* 6, R91–105.
- James, L. C., and Tawfik, D. S. (2001) Catalytic and binding poly-reactivities shared by two unrelated proteins: The potential role of promiscuity in enzyme evolution, *Protein Sci.* 10, 2600–7.
- Wouters, M. A., Liu, K., Riek, P., and Husain, A. (2003) A despecialization step underlying evolution of a family of serine proteases, *Mol. Cell* 12, 343–54.
- Poelarends, G. J., Serrano, H., Johnson, W. H., Jr., Hoffman, D. W., and Whitman, C. P. (2004) The hydratase activity of malonate semialdehyde decarboxylase: mechanistic and evolutionary implications, *J. Am. Chem. Soc.* 126, 15658–9.
- Poelarends, G. J., and Whitman, C. P. (2004) Evolution of enzymatic activity in the tautomerase superfamily: mechanistic and structural studies of the 1,3-dichloropropene catabolic enzymes, *Bioorg. Chem.* 32, 376–92.
- Cheeseman, J. D., Tocilj, A., Park, S., Schrag, J. D., and Kazlauskas, R. J. (2004) Structure of an aryl esterase from *Pseudomonas fluorescens*, *Acta Crystallogr., Sect. D: Biol. Crystallogr.* 60, 1237–43.
- Yew, W. S., Akana, J., Wise, E. L., Rayment, I., and Gerlt, J. A. (2005) Evolution of enzymatic activities in the orotidine 5'-monophosphate decarboxylase suprafamily: enhancing the promiscuous D-arabino-hex-3-ulose 6-phosphate synthase reaction catalyzed by 3-keto-L-gulonate 6-phosphate decarboxylase, *Biochemistry* 44, 1807–15.
- Yew, W. S., Wise, E. L., Rayment, I., and Gerlt, J. A. (2004) Evolution of enzymatic activities in the orotidine 5'-monophosphate decarboxylase suprafamily: mechanistic evidence for a proton relay system in the active site of 3-keto-L-gulonate 6-phosphate decarboxylase, *Biochemistry* 43, 6427–37.
- Miller, B. G., and Raines, R. T. (2004) Identifying latent enzyme activities: substrate ambiguity within modern bacterial sugar kinases, *Biochemistry* 43, 6387–92.
- Schmidt, D. M., Mundorff, E. C., Dojka, M., Bermudez, E., Ness, J. E., Govindarajan, S., Babbitt, P. C., Minshall, J., and Gerlt, J. A. (2003) Evolutionary potential of (beta/alpha)8-barrels: functional promiscuity produced by single substitutions in the enolase superfamily, *Biochemistry* 42, 8387–93.
- Gerlt, J. A., and Babbitt, P. C. (2001) Divergent evolution of enzymatic function: mechanistically diverse superfamilies and functionally distinct suprafamilies, *Annu. Rev. Biochem.* 70, 209–46.
- Farber, G. K., and Petsko, G. A. (1990) The evolution of alpha/beta barrel enzymes, *Trends Biochem. Sci.* 15, 228–34.
- Nagano, N., Hutchinson, E. G., and Thornton, J. M. (1999) Barrel structures in proteins: automatic identification and classification including a sequence analysis of TIM barrels, *Protein Sci.* 8, 2072–84.
- Gerlt, J. A., and Raushel, F. M. (2003) Evolution of function in (beta/alpha)8-barrel enzymes, *Curr. Opin. Chem. Biol.* 7, 252–64.
- Seibert, C. M., and Raushel, F. M. (2005) Structural and Catalytic Diversity within the Amidohydrolase Superfamily, *Biochemistry* 44, 6383–91.
- Holm, L., and Sander, C. (1997) An evolutionary treasure: unification of a broad set of amidohydrolases related to urease, *Proteins* 28, 72–82.
- Donarski, W. J., Dumas, D. P., Heitmeyer, D. P., Lewis, V. E., and Raushel, F. M. (1989) Structure-activity relationships in the hydrolysis of substrates by the phosphotriesterase from *Pseudomonas diminuta*, *Biochemistry* 28, 4650–5.
- Dumas, D. P., Caldwell, S. R., Wild, J. R., and Raushel, F. M. (1989) Purification and properties of the phosphotriesterase from *Pseudomonas diminuta*, *J. Biol. Chem.* 264, 19659–65.
- Omburo, G. A., Kuo, J. M., Mullins, L. S., and Raushel, F. M. (1992) Characterization of the zinc binding site of bacterial phosphotriesterase, *J. Biol. Chem.* 267, 13278–83.
- Shim, H., Hong, S. B., and Raushel, F. M. (1998) Hydrolysis of phosphodiester through transformation of the bacterial phosphotriesterase, *J. Biol. Chem.* 273, 17445–50.
- diSioudi, B., Grimsley, J. K., Lai, K., and Wild, J. R. (1999) Modification of near active site residues in organophosphorus hydrolase reduces metal stoichiometry and alters substrate specificity, *Biochemistry* 38, 2866–72.
- Roodveldt, C., and Tawfik, D. S. (2005) Directed evolution of phosphotriesterase from *Pseudomonas diminuta* for heterologous expression in *Escherichia coli* results in stabilization of the metal-free state, *Protein Eng., Des. Sel.* 18, 51–58.
- Raushel, F. M., and Holden, H. M. (2000) Phosphotriesterase: an enzyme in search of its natural substrate, *Adv. Enzymol. Relat. Areas Mol. Biol.* 74, 51–93.
- Buchbinder, J. L., Stephenson, R. C., Dresser, M. J., Pitera, J. W., Scanlan, T. S., and Fletterick, R. J. (1998) Biochemical characterization and crystallographic structure of an *Escherichia coli* protein from the phosphotriesterase gene family, *Biochemistry* 37, 5096–106.
- Scanlan, T. S., and Reid, R. C. (1995) Evolution in action, *Chem. Biol.* 2, 71–5.
- Porter, T. N., Li, Y., and Raushel, F. M. (2004) Mechanism of the dihydroorotase reaction, *Biochemistry* 43, 16285–92.



28. Matsumura, I., and Ellington, A. D. (2001) *In vitro* evolution of beta-glucuronidase into a beta-galactosidase proceeds through non-specific intermediates, *J. Mol. Biol.* 305, 331–9.
29. Aharoni, A., Gaidukov, L., Khersonsky, O., Mc, Q. G. S., Roodveldt, C., and Tawfik, D. S. (2005) The “evolvability” of promiscuous protein functions, *Nat. Genet.* 37, 73–6.
30. Washabaugh, M. W., and Collins, K. D. (1984) Dihydroorotase from *Escherichia coli*. Purification and characterization, *J. Biol. Chem.* 259, 3293–8.
31. Vartanian, J. P., Henry, M., and Wain-Hobson, S. (1996) Hypermutagenic PCR involving all four transitions and a sizeable proportion of transversions, *Nucleic Acids Res.* 24, 2627–31.
32. Zaccolo, M., Williams, D. M., Brown, D. M., and Gherardi, E. (1996) An approach to random mutagenesis of DNA using mixtures of triphosphate derivatives of nucleoside analogues, *J. Mol. Biol.* 255, 589–603.
33. Stemmer, W. P. (1994) DNA shuffling by random fragmentation and reassembly: *in vitro* recombination for molecular evolution, *Proc. Natl. Acad. Sci. U.S.A.* 91, 10747–51.
34. Gould, S. M., and Tawfik, D. S. (2005) Directed evolution of the promiscuous esterase activity of carbonic anhydrase II, *Biochemistry* 44, 5444–52.
35. Aharoni, A., Gaidukov, L., Yagur, S., Toker, L., Silman, I., and Tawfik, D. S. (2004) Directed evolution of mammalian paraoxonases PON1 and PON3 for bacterial expression and catalytic specialization, *Proc. Natl. Acad. Sci. U.S.A.* 101, 482–7.
36. Khalameyzer, V., Fischer, I., Bornscheuer, U. T., and Altenbuchner, J. (1999) Screening, nucleotide sequence, and biochemical characterization of an esterase from *Pseudomonas fluorescens* with high activity towards lactones, *Appl. Environ. Microbiol.* 65, 477–82.
37. Fersht, A. (2000) *Structure and Mechanism in Protein Science*, 2000 ed., W. H. Freeman and Company, New York.
38. Hong, S. B., and Raushel, F. M. (1996) Metal-substrate interactions facilitate the catalytic activity of the bacterial phosphotriesterase, *Biochemistry* 35, 10904–12.
39. Reardon, D., and Farber, G. K. (1995) The structure and evolution of alpha/beta barrel proteins, *FASEB J.* 9, 497–503.
40. Benning, M. M., Shim, H., Raushel, F. M., and Holden, H. M. (2001) High-resolution X-ray structures of different metal-substituted forms of phosphotriesterase from *Pseudomonas diminuta*, *Biochemistry* 40, 2712–22.
41. Aubert, S. D., Li, Y., and Raushel, F. M. (2004) Mechanism for the hydrolysis of organophosphates by the bacterial phosphotriesterase, *Biochemistry* 43, 5707–15.
42. Yang, H., Carr, P. D., McLoughlin, S. Y., Liu, J. W., Horne, I., Qiu, X., Jeffries, C. M., Russell, R. J., Oakeshott, J. G., and Ollis, D. L. (2003) Evolution of an organophosphate-degrading enzyme: a comparison of natural and directed evolution, *Protein Eng.* 16, 135–45.
43. Mesecar, A. D., Grimsley, J. K., Holton, T., and Wild, J. R. (2003) (pdb: 1qw7) Unpublished results.
44. Benning, M. M., Kuo, J. M., Raushel, F. M., and Holden, H. M. (1994) Three-dimensional structure of phosphotriesterase: an enzyme capable of detoxifying organophosphate nerve agents, *Biochemistry* 33, 15001–7.
45. Benning, M. M., Hong, S. B., Raushel, F. M., and Holden, H. M. (2000) The binding of substrate analogs to phosphotriesterase, *J. Biol. Chem.* 275, 30556–60.
46. Jurgens, C., Strom, A., Wegener, D., Hettwer, S., Wilmanns, M., and Sterner, R. (2000) Directed evolution of a (beta alpha)8-barrel enzyme to catalyze related reactions in two different metabolic pathways, *Proc. Natl. Acad. Sci. U.S.A.* 97, 9925–30.
47. Joerger, A. C., Mayer, S., and Fersht, A. R. (2003) Mimicking natural evolution *in vitro*: an N-acetylneuraminase lyase mutant with an increased dihydrodipicolinate synthase activity, *Proc. Natl. Acad. Sci. U.S.A.* 100, 5694–9.
48. Graham, L. D., Haggett, K. D., Jennings, P. A., Le Brocq, D. S., Whittaker, R. G., and Schober, P. A. (1993) Random mutagenesis of the substrate-binding site of a serine protease can generate enzymes with increased activities and altered primary specificities, *Biochemistry* 32, 6250–8.
49. Yano, T., Oue, S., and Kagamiyama, H. (1998) Directed evolution of an aspartate aminotransferase with new substrate specificities, *Proc. Natl. Acad. Sci. U.S.A.* 95, 5511–5.
50. Zhang, J. H., Dawes, G., and Stemmer, W. P. (1997) Directed evolution of a fucosidase from a galactosidase by DNA shuffling and screening, *Proc. Natl. Acad. Sci. U.S.A.* 94, 4504–9.

BI051021E